Insights into thermal degradation of organic light emitting diodes induced by glass transition through impedance spectroscopy

G. Nenna,[1,a)] M. Barra,[2] A. Cassinese,[2,3] R. Miscioscia,[1] T. Fasolino,[1] P. Tassini,[1] C. Minarini,[1] and D. della Sala[4]
[1]*FIM-MAT Nano, Portici ENEA Research Center, P.le Enrico Fermi, 80055 Portici, Naples, Italy*
[2]*Dipartimento di Fisica and CNR-INFM Coherentia, Università di Napoli Federico II, Naples, Italy*
[3]*Technological District, IMAST Scarl, Loc. Granatello, Portici, Naples, Italy*
[4]*FIM-MAT Nano, Casaccia ENEA Research Center, Via Anguillarese 301, 00123 S. M. di Galeria, Roma, Italy*

(Received 27 February 2009; accepted 13 May 2009; published online 19 June 2009)

Highly sensitive alternate current (ac) impedance measurements with variable temperature have been performed to investigate the optical and electrical failure mechanisms during the glass transition phenomena in the archetypal ITO/TPD/Alq_3/Al organic light emitting diode (OLED) structure. Since the device degradation is mainly related to the lower glass transition temperature (T_g) of the N,N'-Bis(3-methylphenyl)-N,N'-diphenylbenzidine (TPD), this study is focused on the frequency response of thin TPD films approaching the glassy region. The related experimental data are discussed in the framework of the universal dielectric response model. By ac measurements, TPD glass transition temperature is located and temperature regions with different OLED behaviors are evidenced. The relation between the behaviors of TPD frequency response and of the OLED electro-optical response, while the temperature approaches the glass transition region, is discussed.
 [DOI: 10.1063/1.3151705]

I. INTRODUCTION

Operational stability of organic light emitting diodes (OLEDs) is undoubtedly the most important issue to establish their potential commercial applications.[1] Among other reasons, thermal effects causing irreversible material degradation can play a crucial role in defining the device operation limits, when large current densities are produced and self-heating phenomena have to be considered.[2] In this regard, many studies have been reported showing how an OLED differently behaves during its lifetime at various working regimes and at different substrate temperatures.[3–6] Hence, several strategies have been adopted in the attempt to reduce thermal aging effects.[4,5]

So far, high temperature stability studies have been mainly devoted to analyze thermally induced morphological changes in the organic materials[3,7] and to determine the critical temperatures above which the devices finally fail.[4–6,8,9] More in detail, it has been demonstrated that one the major thermal effects producing OLED degradation is basically related to the morphological instability of the hole transport layer (HTL), as temperature approaches its glass transition.[10–12] Despite the considerable interest for this subject, still today, quantitative correlations between the glass transition occurrence and the device operating limits are not well established.[7,13,14] Recently, it has been shown that alternate current (ac) electrical measurements performed at different temperatures represent a reliable and not destructive tool to investigate the glass transition phenomenon in device operational situations.[11,15] These measurements are based on the application of small alternate signals (amplitude ≤ 1 V); thus preventing direct self-heating effects and related self-induced aging mechanisms. Furthermore, differently from other electrical techniques, they do not require doping procedures to increase the basic conductivity of the investigated material.[11]

In this paper, the glass transition phenomenon and its effects on the electro-optical response of a basic OLED structure are investigated by high sensitivity ac measurements. For our purposes, a very simple and well referred OLED configuration (ITO/TPD/Alq_3/Al) has been considered,[16–18] neglecting at moment the insertion of any injection layers that could further complicate the analysis of the device frequency response. TPD was selected for its low and well known glass transition temperature, involving morphological changes which affect the device overall behavior without directly damaging the emitter material (Alq_3). The frequency response of N,N'-Bis(3-methylphenyl)-N,N'-diphenylbenzidine (TPD) thin films has been analyzed as a function of temperature and, consequently, modeled according to the main parameters of the so-called universal dielectric response model (UDR). Characteristic temperature values are experimentally extracted and correlated with the different electro-optical operation regions of the OLED. The main target of this study is to clarify the underlying physical mechanisms related to the operation failure of OLEDs approaching the glassy region.

II. EXPERIMENTAL

Three basic device configurations (see Fig. 1) have been fabricated on Corning 1737 glass substrates deposited with commercial 200 nm thick indium tin oxide (ITO) layer (sheet

[a)]Author to whom correspondence should be addressed. Electronic mail: giuseppe.nenna@enea.it. Tel.: +39 0817723410.

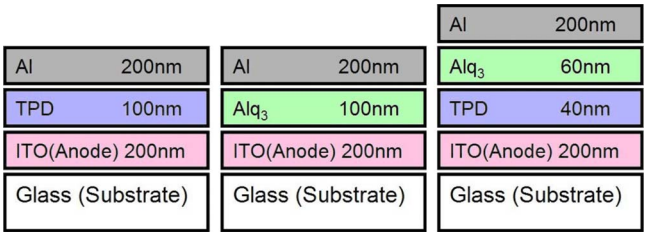

FIG. 1. (Color online) The devices considered in this work: on the left, ITO/TPD/Al device (a); in the middle, ITO/Alq_3/Al device (b); and on the right, ITO/TPD/Alq_3/Al device (c).

resistance $R_s \approx 10\ \Omega/\square$). Single organic layer devices (A and B) have been realized by depositing separately a 100 nm thick film of TPD and Alq_3, respectively. For the last device (C), a basic double layer OLED configuration has been adopted, with a 40 nm thick TPD film as HTL and a 60 nm thick Alq_3 film as electron transport layer (ETL) and as emissive layer. In any case, an aluminum (Al) cathode has been evaporated to complete the device structure. The active area of each device is 12.56 mm^2.

The substrates have been cleaned with de-ionized water, detergent and ultrasounds. Then, they have been dried in oven at 115 °C for 2 h. The ITO anodes have been patterned through photolithography and HCl-based solution etching. The organic layers have been thermally evaporated sequentially without patterning and, when it has been necessary, there was no vacuum breaking between their depositions. The base vacuum was always between 10^{-6} and 10^{-7} mbar and the growth rates for the organic layers have been between 1 and 2 Å/s. The Al cathode has been evaporated through shadow mask, with growth rate of about 2 and 3 Å/s.

All measurements have been performed in vacuum ($P \approx 10^{-4}$ mbar), mounting the sample in a cryostat with optical windows. Variable temperature experiments were carried out with a rate of about 0.5 K/min. ac measurements (amplitude ac voltage of 1 V) have been performed by using an Agilent LCR meter. The investigated frequency and temperature ranges are [100–100 KHz] and (300–360) K, respectively. ac experimental setup has guaranteed a resolution for the equivalent capacitance and conductance measurements of about 0.1 pF and 1×10^{-10} S, respectively.[10,15] Direct current (dc) current-voltage (*I-V*) measurements have been performed by a Keithley 2400 power supply source meter in voltage mode, with constant increment steps and delay time of 1 s before each measurement point. An integrating sphere and a photodiode (Newport 810UV) connected to a Keithley 6517A electrometer have been employed for the electroluminescence (EL) analysis.

III. RESULTS

A. OLED dc characterization

To investigate the operational limits of our basic OLED structure, current-voltage (*I-V*) and EL-voltage (EL-V) measurements have been performed at increasing driving voltages, until the device electrical and optical breakdown. Figure 2 clearly shows that, as a function of the applied voltage,

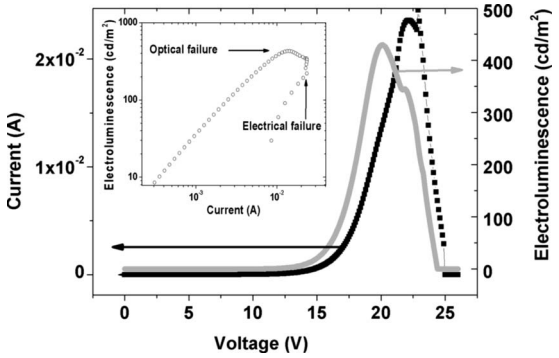

FIG. 2. Typical *I-V* and EL-V characteristics for an ITO/TPD/Alq_3/Al device. (Inset) Plot of EL vs device current, displaying both optical and electrical failures.

both current and EL get a maximum value before rapidly decreasing. In any case, the experimental findings reveal that the "optical failure" occurs at lower voltages (about 20 V) in comparison with the "electrical failure" (about 22 V).

A complementary picture of this situation is given in the inset of Fig. 2, where the EL is plotted versus the device current and the different failure events are more directly evidenced. Infrared (IR) imaging analyses, carried out in the same operating conditions, highlight the occurrence of very complex thermal scenarios inside the device, involving a very large temperature gradient (about 40 K) and maximum temperature values up to 360 K.[8,9] Consequently, a clear and quantitative correlation between the device behavior and the glass transition effects has been shown to be not possible by IR measurements alone.

To gain more insights on this feature, an alternative procedure has been followed, driving the OLED at a fixed voltage (15 V) and forcing externally the device temperature by a resistive heater. This driving voltage has been chosen to be higher than the optical onset voltage but considerably lower than breakdown values, in order to limit the self-heating effects. In this way, the behaviors of device current and of EL both versus temperature have been accurately monitored up to 360 K (Fig. 3). As expected, both the current and the luminescence display temperature dependences, with peculiar features concentrated above 330 K.

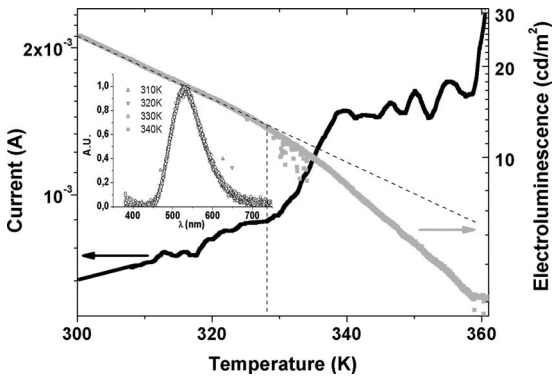

FIG. 3. Electroluminescence and device current as function of temperature for the TPD/Alq_3 OLED device at $V=15$ V. (Inset) Device spectra (arbitrary unit) vs temperature.

In these curves, three main regions can be identified. In the first one, from room temperature to about 328 K, device current increases according to a conventional thermal activation law. On the other hand, the corresponding EL slight reduction has to be attributed to the inevitable underlying device degradation in time, mainly affecting the emission properties.[19,20]

The starting value (about 328–329 K) of the second zone is marked by a clear change in the slope of both EL and *I* curves. In detail, EL starts to decrease more rapidly, and in a complementary way a faster increase in the device current takes place. This can be interpreted in terms of a significant increase in hole traps concentration near the HTL/ETL interface, which can easily act as recombination centers with a dominant nonradiative behavior.[2] Furthermore, a contemporaneous spectral analysis, performed by a spectrum-radiometer and reported in the inset in Fig. 3, allows confirming that EL variation is related only to the intensity of emitted light and not to spectrum modification. It is important to outline that TPD T_g value usually reported in literature is located between 333 and 338 K, meaning that the device response in the second region should be the most significantly affected by glass transition occurrence.[14,21,22]

Finally, the third region starts at about 341 K, where the current begins displaying an unstable behavior with significant negative differential resistance zones. Here, TPD has completely changed its phase and the overall device behavior should be slightly masked by the presence of Alq_3 layer, until the definitive failure at about $T \sim 360$ K.[8,9]

B. OLED and TPD device frequency response

In order to investigate the basic physical phenomena underlying the OLED temperature features evidenced in the previous section, ac impedance measurements have been performed for all the device configurations shown in Fig. 1. Our analysis has been limited to the temperature range between room temperature and 343 K, being mainly focused on the TPD glass transition effects. For TPD devices, ac measurements at higher temperatures (up to 360 K) have shown the occurrence of electrical instabilities (sample dependent), with large and irreversible low frequency conductivity switching. A detailed discussion of these effects, generally attributed to extrinsic phenomena related to the device mechanical/structural fail, is out of the scope of this work.

Figure 4 reports a comparison of the real part (ReZ) of the measured impedances for three typical devices A, B, and C for a temperature variation from 297 to 343 K. For device A (single TPD layer), two orders of magnitude change can be appreciated for ReZ by increasing the temperature, while, in comparison, a very small evolution can be noted for the Alq_3 device (B) in the same range. Obviously, this different temperature sensitivity is due to the TPD glass transition occurrence, being Alq_3 T_g located at much higher temperatures.[21] In similar way, the presence of Alq_3 in device C seems to mask the TPD temperature behavior, reducing the corresponding ReZ increase.

Provided those results, in the following, our attention is focused on the analysis of the device A (ITO/TPD/Al) frequency response and on its temperature dependence. To this regard, the corresponding variable temperature real and imaginary parts of the impedance are reported in Fig. 5. This figure makes clear that variation of ReZ along temperature becomes actually significant above 330 K, while no appreciable change can be detected from the imaginary part (–*X*) data, showing an almost constant slope as a function of frequency. By this last occurrence, it is possible to conclude that a simple circuit with a single *RC* parallel loop and a series resistance R_s (30–40 Ω), modeling the ReZ high frequency ($f > 20$ kHz) plateau, is suitable to describe the device A frequency response in all the investigated temperature range.[23] Furthermore, the R_s slight lowering at increasing temperatures reveals that it can be mainly due to the ITO anode contact. In order to focus the attention only on the temperature dependence of TPD intrinsic electrical properties, the R_s contribution has been subtracted from frequency data and a conductance/capacitance parallel mode representation has been adopted, directly accounting for TPD conductivity and dielectric permittivity (Fig. 6). Anyway, hereafter, the data analysis will be referred to the frequency range between 100 Hz and 10 kHz, where any residual contact resistance contribution can be excluded.

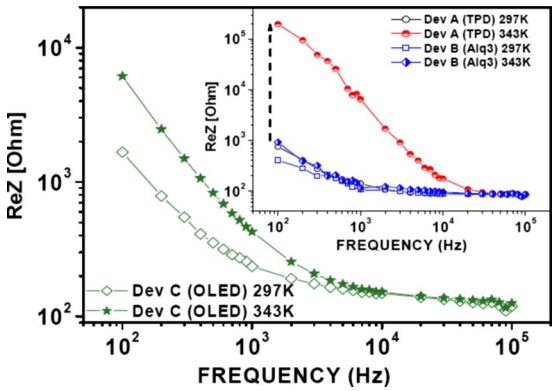

FIG. 4. (Color online) Real part of the impedance (ReZ) for device C and (inset) for devices A and B, measured at 297 and 343 K.

As shown, conductance (*G*) and capacitance (*C*) follow a complementary behavior: the former increases with temperature while the latter decreases. Moreover, the conductance variation rate gets more pronounced approaching the

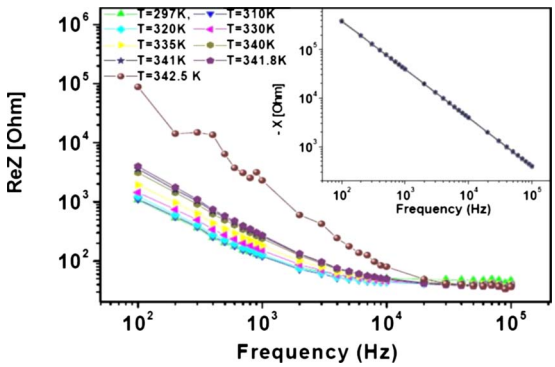

FIG. 5. (Color online) Real part of impedance (ReZ) measured at different temperatures for device A. In the inset, the corresponding imaginary part (–*X*).

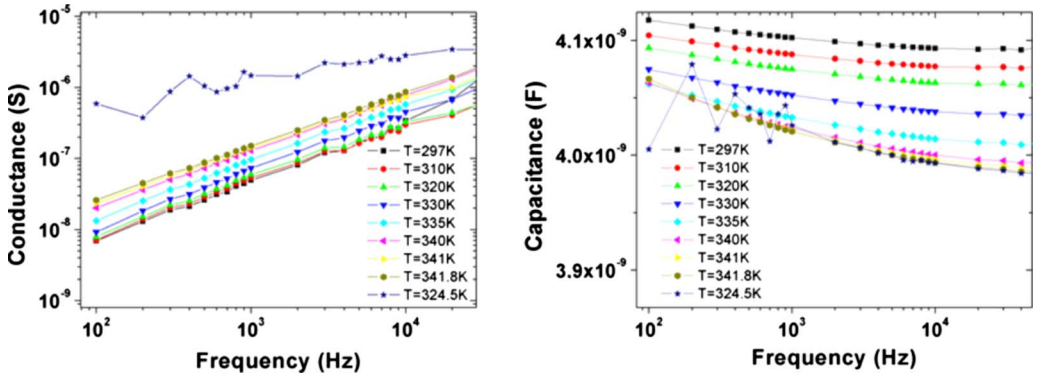

FIG. 6. (Color online) Conductance (left) and capacitance (right) as a function of frequency, measured at different temperatures.

upper temperature limit (343 K), while the capacitance behavior seems much more complex and depending on frequency. It should also be noted that low frequency experimental data appear noticeably scattered close to 343 K for both capacitance and conductance. Anyway, no irreversible effect is detected below this value.

The frequency dependence of conductance in the log-log plot suggests that experimental data can be well described by the UDR model,[24,25] which for G predicts the expression:

$$G(\omega) = G_0 + A_G * \omega^s. \tag{1}$$

Here, A_G is the constant phase element that shows dispersion of conductivity and dielectric properties of the filling material,[26] while G_0 is basically related to the conductivity in the limit $\omega \rightarrow 0$. Usually, the exponent s allows classifying empirically the electrical nature of the investigated disordered materials: s was experimentally demonstrated to be close to 0.8 (Ref. 27) or 1 (Ref. 28) for amorphous semiconductors and insulators, respectively.

By using Eq. (1), temperature dependence of the s parameter has been extracted from conductance data in Fig. 6 and it is reported in Fig. 7. As shown, s results to be close to 0.8 and displays weak temperature dependence, with a more pronounced reduction only near 340 K and a final drop in the 343 K proximity. In general, s decreasing behavior at increasing temperature is expected in organic compounds, where basic hopping mechanisms rule the conduction processes.[29] Here, we want also to stress that R_s subtraction from impedance data is essential for the correct evaluation of s which, otherwise, could be estimated even greater than 1.

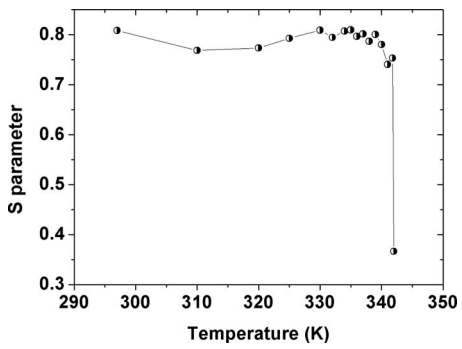

FIG. 7. UDR s parameter as a function of temperature.

In order to relate more directly the ac measurements on TPD-only devices with the OLED temperature behavior, capacitance and conductance data have been plotted as a function of temperature for frequencies in the range between 100 Hz and 1 kHz (Fig. 8). This representation helps to clearly identify characteristic temperature regions, resembling those evidenced in the OLED response analysis.

At each frequency, approaching 343 K, conductance increases with temperature, according to a law given by the superimposition of more than exponential behaviors. On the contrary, capacitance linearly decreases from room temperature up to about 320 K, independently on frequency. In this temperature range, in a first approximation, the capacitance reduction can be completely ascribed to the TPD thermal expansion that allows an estimation of the related coefficient by the expressions:

$$\Delta C = \varepsilon_0 \varepsilon_r \frac{A}{\Delta d} \quad \text{and} \quad \frac{\Delta d}{d_0} = \alpha^* \Delta T, \tag{2}$$

where d_0 is the starting TPD thickness. By this simple approach, α has been estimated to be about 2.57×10^{-4} K^{-1} which is similar to the value evaluated by x-ray reflectivity measurements.[21]

Above 320 K, capacitance behavior becomes much more frequency dependent and is no longer monotonically decreasing. In particular, at the lowest frequencies (100 and 200 Hz), C reveals the occurrence of a minimum between 335 and 338 K, where T_g is located. Furthermore, it is possible to observe that at higher frequencies the capacitance minimum tends to shift to higher temperatures, in agreement with T_g frequency dependence.[11] Hence, by these observations, it seems that the incoming molecular rearrangement toward to the new quasiglassy state and the related variation in the material viscosity find a direct manifestation in the temperature-dependent dielectric relaxation. A more concise representation of C and G data is proposed in Fig. 9, where the ratio between C and G is reported as a function of temperature at different frequencies.

The resultant RC dispersive behavior, with its significant frequency dependence, is another direct consequence of the UDR model. By these data, temperatures around 328–329 K still appear as a separation point between two different working regimes. Anyway, in both the two ranges, RC data display linear temperature dependences with two different

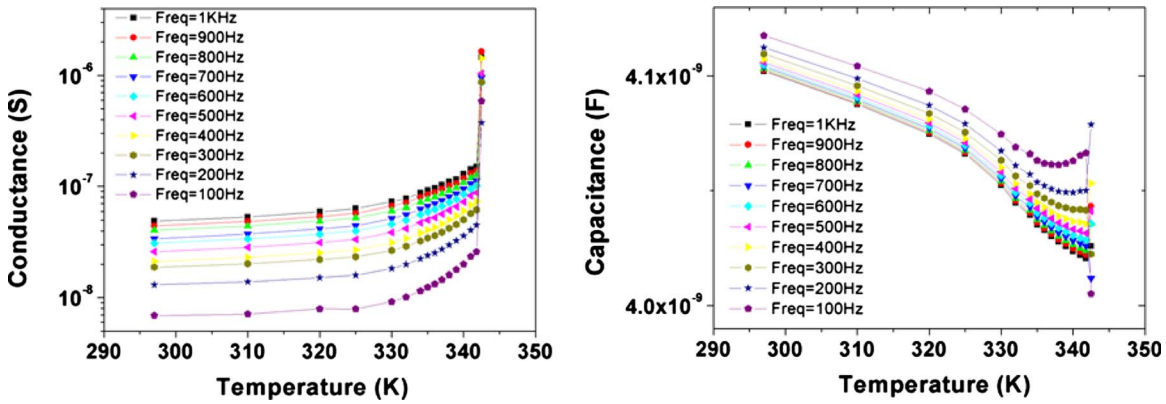

FIG. 8. (Color online) Temperature-dependent conductance (left) and capacitance (right) for the device A at different working frequencies.

slopes. These experimental findings relate definitively the OLED electro-optical response in the temperature range between 328 and 340 K to the TPD behavior and to the occurrence of the glass transition. In more detail, we infer that the slope changes in the OLED EL and current occurring at 328–329 K can be related to glass transition effects mainly involving the interface regions between HTL and ETL, and HTL and the anode. Although our measurements account for a glass transition occurrence in the bulk material located between 335 and 338 K, T_g interface localized effects at lower temperatures cannot be excluded,[30] pointing out for more care in the definition of device operational limits. Further experiments considering OLED with different HTL layer thickness are envisaged. In any case, OLED behavior above 340 K is strongly affected by the TPD glassy state which introduces remarkable current perturbation and makes more critical the role of ETL layer.

IV. CONCLUSIONS

In this work, the ac electrical response of thin TPD films approaching the glass transition region has been investigated. The results analysis shows that the glass transition occurrence has a strong impact on the electro-optical behavior of an OLED based on TPD HTL, defining different working regimes. In particular, glass transition kinetics seems to involve a temperature range of about 10 K below the nominal glass transition temperature. Interface effects have to be considered to this concern. ac impedance spectroscopy coupled with thermal stress has confirmed to be a useful technique to study the processes governing the dynamics of glass transition and a tool to evidence the device operational limitations.

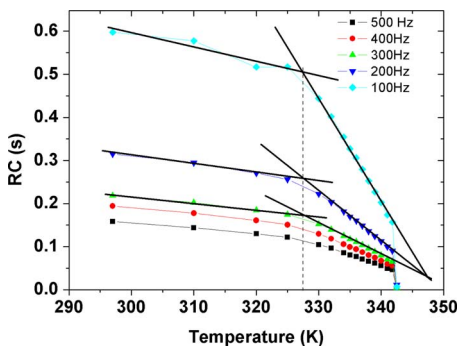

FIG. 9. (Color online) *RC* data vs temperature at different working frequencies.

ACKNOWLEDGMENTS

This research is financially supported by MIUR-TRIPODE (Contract No. DM 20160) project. The technical support of A. Maggio, S. Marrazzo, P. D'Angelo, E. Calò, and P. Vacca is gratefully acknowledged.

[1] R. S. Cok and F. A. Leon, U.S. Patent No. 7158106 (12 January 2005).
[2] D. Y. Kondakov, J. R. Sandifer, C. W. Tang, and R. H. Young, J. Appl. Phys. **93**, 1108 (2003).
[3] D. H. Chung, S. W. Hur, S. K. Kim, J. U. Lee, C. H. Kim, J. W. Hong, and T. W. Kim, Curr. Appl. Phys. **4**, 667 (2004).
[4] D. F. O'Brian, P. E. Burrows, S. R. Forrest, B. E. Koene, D. E. Loy, and M. E. Thompson, Adv. Mater. (Weinheim, Ger.) **14**, 1108 (1998).
[5] G. Vamvounis, H. Aziz, N.-X. Hub, and Z. D. Popovic, Synth. Met. **143**, 69 (2004).
[6] P. N. M. dos Anjos, H. Aziz, N. X. Hu, and Z. D. Popovic, Org. Electron. **3**, 9 (2002).
[7] V. I. Adamovich, M. S. Weaver, R. C. Kwong, and J. J. Brown, Curr. Appl. Phys. **5**, 15 (2005).
[8] G. Nenna, G. Flaminio, T. Fasolino, C. Minarini, R. Miscioscia, D. Palumbo, and M. Pellegrino, Macromol. Symp. **247**, 326 (2007).
[9] X. Zhou, J. He, L. S. Liao, M. Lu, X. M. Ding, X. Y. Hou, X. M. Zhang, X. Q. He, and S. T. Lee, Adv. Mater. (Weinheim, Ger.) **12**, 265 (2000).
[10] L. E. Nielsen, *Mechanical Properties of Polymers and Composites* (Dekker, New York, 1974), Vol. 1.
[11] P. D'Angelo, M. Barra, M. Nicodemi, and A. Cassinese, J. Appl. Phys. **101**, 044910 (2007).
[12] J. A. Quintana, P. G. Boj, J. M. Villalvilla, M. A. Díaz-García, J. Ortiz, L. Martín-Gomis, F. Fernández-Lázaro, and Á. Sastre-Santos, Appl. Phys. Lett. **92**, 041101 (2008).
[13] K. A. Osipov, V. N. Pavlovskii, E. V. Lutsenko, A. L. Gurskii, G. P. Yablonskii, S. Hartmann, A. Janssen, H.-H. Johannes, R. Caspary, W. Kowalsky, N. Meyer, M. Gersdorff, M. Heuken, P. van Gemmern, C. Zimmermann, F. Jessen, H. Kalisch, and R. H. Jansen, Thin Solid Films **515**, 4834 (2007).
[14] S. Tokito, H. Tanaka, K. Noda, A. Okada, and Y. Taga, IEEE Trans. Electron Devices **44**, 1239 (1997).
[15] A. Castaldo, L. Quercia, G. Di Francia, A. Cassinese, and P. D'Angelo, J. Appl. Phys. **103**, 054511 (2008).
[16] G. E. Jabbour, B. Kippelen, N. R. Armstrong, and N. Peyghambarian, Appl. Phys. Lett. **73**, 31 (1998).
[17] H. Mu, H. Shen, and D. Klotzkin, Solid-State Electron. **48**, 2085 (2004).
[18] Z. S. X. Junqing, S. Han, Z. Yang, L. Ye, and T. Yang, Phys. Status Solidi A **184**, 233 (2001).
[19] S. Y. Kim, K. Y. Kim, Y.-H. Tak, and J.-L. Lee, Appl. Phys. Lett. **89**, 132108 (2006).
[20] P. E. Burrows, V. Bulovic, S. R. Forrest, L. S. Sapochak, D. M. McCarty, and M. E. Thompson, Appl. Phys. Lett. **65**, 2922 (1994).

[21]P. Fenter, F. Schreiber, V. Bulovid, and S. R. Forrest, Chem. Phys. Lett. **277**, 521 (1997).
[22]J. Xu and B. Chen, J. Mol. Model. **12**, 24 (2005).
[23]M. Barra, P. D'Angelo, A. Cassinese, L. E. Hueso, P. Graziosi, and V. Dediu, Org. Electron. **9**, 911 (2008).
[24]A. K. Jonscher, IEEE Electr. Insul. Mag. (USA) **6**, 16 (1990).
[25]M. Barra, M. Biasiucci, A. Cassinese, P. D'Angelo, A. C. Barone, A. Carella, and A. Roviello, J. Appl. Phys. **102**, 093712 (2007).
[26]Z. G. Zhang, D. P. Chu, and M. McGregor, Appl. Phys. Lett. **83**, 2892 (2003).
[27]M. Pollak and T. H. Geballe, Phys. Rev. **122**, 1742 (1961)
[28]A. K. Jonscher, IEEE Trans. Electr. Insul. **27**, 407 (1992).
[29]S. R. Elliott, Adv. Phys. **36**, 135 (1987).
[30]C. Kim, A. Facchetti, and T. J. Marks, Science **318**, 76 (2007).